



# Unveiling the nature of thermonuclear runaway supernovae with radio observations

Javier Moldón<sup>1</sup>, Miguel Á. Pérez-Torres<sup>1,2,3</sup>, Erik C. Kool<sup>4,5,6</sup>, Seppo Mattila<sup>2,7</sup>, Peter Lundqvist<sup>6</sup>, and Robert J. Beswick<sup>8</sup>

<sup>1</sup> Instituto de Astrofísica de Andalucía, Consejo Superior de Investigaciones Científicas (CSIC), Glorieta de la Astronomía s/n, E-18008 Granada, Spain

<sup>2</sup> School of Sciences, European University Cyprus, Diogenes street, Engomi, 1516 Nicosia, Cyprus

<sup>3</sup> Facultad de Ciencias, Universidad de Zaragoza, Pedro Cerbuna 12, E-50009 Zaragoza, Spain

<sup>4</sup> Finnish Centre for Astronomy with ESO (FINCA), University of Turku, FI-20014 Turku, Finland

<sup>5</sup> Department of Physics and Astronomy, University of Turku, FI-20014 Turku, Finland

<sup>6</sup> The Oskar Klein Centre, Department of Astronomy, Stockholm University, AlbaNova, SE-10691, Stockholm, Sweden

<sup>7</sup> Tuorla Observatory, Department of Physics and Astronomy, University of Turku, FI-20014 Turku, Finland

<sup>8</sup> Jodrell Bank Centre for Astrophysics, School of Physics and Astronomy, The University of Manchester, Manchester M13 9PL, UK

**Abstract.** We present the results of our study on the type Ia supernova 2020eyj, which exhibits helium-rich circumstellar material, as demonstrated by its spectral features and infrared emission. Here, we focus on our e-MERLIN observing campaign on SN 2020eyj, which resulted in the the first-ever radio detection of a SN Ia. Based on our modeling, we conclude that the circumstellar material most likely originates from a single-degenerate binary system in which a white dwarf accretes material from a helium donor star. We briefly discuss this detection in the context of the previous radio upper limits and their implications, and describe in detail how we achieved this remarkable result. We also discuss how a comprehensive radio follow-up of SN 2020eyj-like SNe Ia can improve the constraints on their progenitor systems.

## 1. Introduction

Type Ia supernovae (SNe Ia) are thermonuclear explosions of degenerate white dwarf stars destabilized by mass accretion from a companion star. Despite SNe Ia having been used to unveil the accelerated expansion of the universe, the nature of their progenitors remains poorly understood. To distinguish between a degenerate and non-degenerate progenitor companion, one can use radio observations. A non-degenerate companion star is expected to lose material through winds or binary interaction before the explosion, and the supernova ejecta colliding with this circumstellar material should produce radio synchrotron emission. However, despite extensive efforts, including some of the deepest upper limits ever obtained by our team using e-MERLIN and the EVN (e.g., SN 2014J Pérez-Torres et al. 2014; see also Lundqvist et al. 2020), no type Ia supernova has been detected at radio wavelengths. This suggests a clean environment and a companion star that is itself a degenerate white dwarf.

Type Ia-CSM are a rare subclass of thermonuclear supernovae that strongly interact with their circumstellar medium (CSM). The presence of the CSM implies mass transfer between a non-degenerate donor star and the white dwarf (WD), the so-called single-degenerate SN Ia channel. As such, Type Ia-CSM are strong candidates for the single-degenerate SN Ia channel. The core-collapse vs. thermonuclear nature of SNe Ia-CSM has been hotly

debated in the literature, until the discovery of PTF11kx cemented SNe Ia-CSM as a bona fide subclass (Dilday et al., 2012). This SN was observed to interact with multiple shells of slow-moving CSM, but the CSM interaction was delayed by 50 days, which allowed for a secure SN Ia classification at peak. The CSM-free cavity and the slow-moving shells were interpreted as resulting from a symbiotic nova progenitor, where recurrent novae on the accreting WD swept up the CSM originating from a donor star wind.

A recent analog to PTF11kx is SN 2020eyj<sup>1</sup> (=ZTF20aatxryt), a SN Ia that also shows prominent CSM interaction with a  $\sim 60$ -day delay. This makes it the fourth delayed SN Ia-CSM after. However, unlike any other known SNe Ia-CSM, it interacts with He-rich environment rather than a H-rich. This discovery provides unique observational evidence to the WD + He donor SN Ia channel, a channel that has been extensively studied in the literature as a scenario for short-delay SNe Ia (e.g. Wang et al., 2009).

PTF11kx was observed in the radio at 8.4 GHz, 75 days after explosion, and was not detected. However, Harris et al. (2021) modeled the radio light curve of PTF11kx, based on the framework from Harris et al. (2016) for radio light curves of supernovae interacting with CSM shells, and concluded that an observation at  $\sim 500$  days would have been better suited to detect the

<sup>1</sup> <https://www.wis-tns.org/object/2020eyj>

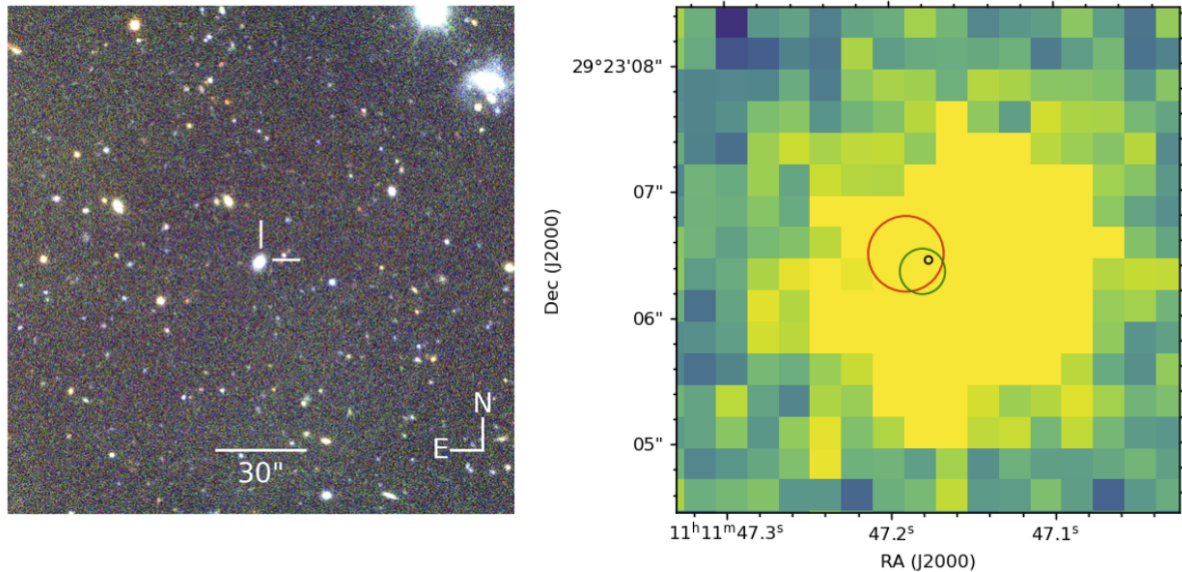


**Fig. 1. The position of the radio detection is consistent with the position of SN 2020eyj in the optical.** Left panel: A  $3' \times 3'$  color composite image, obtained with NOT/ALFOSC, of the compact star-forming host galaxy of SN 2020eyj and its environment. Right panel: The average position of the e-MERLIN detections (black circle,  $0.01''$  uncertainty), the position reported in GaiaAlerts (*G* band, green circle,  $0.06''$  uncertainty), and the position of SN 2020eyj in the ALFOSC epoch at +382 days (*r* band, red circle,  $0.1''$  uncertainty), overlaid on a  $4'' \times 4''$  Pan-STARRS1 *i*-band data of the host. From Kool et al. (2023)

SN, and constrain its CSM properties. SN 2020eyj is relatively nearby (131 Mpc) compared to the other delayed Ia-CSM SNe PTF11kx (207 Mpc), SN 2015cp (167 Mpc) and SN 2002ic (300 Mpc), so this was an excellent candidate for a radio detection.

## 2. e-MERLIN Observations

We observed SN 2020eyj with the electronic Multi-Element Radio Linked Interferometre Network (e-MERLIN) across two distinct observing periods. The initial observation was performed on 2021 November 19 (MJD 59538.29), approximately 605 days post-discovery, utilizing six e-MERLIN antennae (Mk2, Kn, De, Cm, Da and Pi) for a total integration time of  $\sim 16$  hours on the target and phase calibrator. The follow-up observations were conducted across a 6-day period from 2022 April 6-12 (mean MJD 59678.59, +741 days post-discovery), employing 5-6 telescopes including the Lovell telescope, with occasional antenna downtime due to technical issues. To accommodate the Lovell telescope restricted field of view, we offset the pointing center by 1 arcmin during the second epoch to ensure an in-beam calibrator remained within its primary beam.

The observational setup utilized 3C 286 and OQ 208 as the amplitude and bandpass calibrators respectively. We observed J1106+2812 ( $\alpha_{J2000.0} = 11^{\text{h}}06^{\text{m}}07.2617^{\text{s}}$ ,  $\delta_{J2000.0} = 28^{\circ}12' 47.065''$ ) as our phase calibrator, located  $1.7^{\circ}$  from the target, with a measured flux density of 150 mJy. Observations were configured at a central frequency of 5.1 GHz with a 512 MHz bandwidth. Data correlation was performed at Jodrell Bank Observatory

(JBO) using the e-MERLIN correlator, configured with 4 spectral windows (512 channels each), 1-second integration time, and full polarization capabilities. Data reduction employed the e-MERLIN CASA pipeline Moldon (2021) v1.1.19 implemented in CASA 5.6.2. Phase and amplitude self-calibration was achieved using a 10 mJy inbeam source. Image reconstruction was performed using `wsclean` (Offringa et al., 2014). The resulting synthesized beams measured  $80 \text{ mas} \times 35 \text{ mas}$  (P.A.  $28^{\circ}$ ) and  $94 \text{ mas} \times 71 \text{ mas}$  (P.A.  $-71^{\circ}$ ) for the first and second epochs respectively, achieving noise levels of 17 and  $8 \mu\text{Jy beam}^{-1}$ . The target was detected as an unresolved source in both epochs using IMFIT. Source flux densities were measured at  $80 \pm 20$  and  $60 \pm 10 \mu\text{Jy beam}^{-1}$  for the respective epochs, with uncertainties incorporating both the image rms and a conservative 10% amplitude calibration uncertainty. The radio emission was localized to  $\alpha_{J2000.0} = 11^{\text{h}}11^{\text{m}}47.1763^{\text{s}}$ ,  $\delta_{J2000.0} = 29^{\circ}23'06.45''$ , with a positional uncertainty of 10 mas. Fig. 1 displays the mean e-MERLIN position relative to the optical coordinates of SN 2020eyj. The radio detection shows positional agreement with both the ALFOSC *r*-band observation at +382 days and the GaiaAlerts<sup>2</sup> *G*-band detection at +42 days. SN 2020eyj exploded in a low-luminosity star-forming dwarf galaxy (Kool et al., 2023). The e-MERLIN localization puts the source in the outskirts of the host galaxy (see Fig. 1-right), without any other obvious potential counterparts. At the distance of the host galaxy, the 50 mas compact source would have maximum size of 30 pc. Given this context, and the spatial coincidence with

<sup>2</sup> <http://gsaweb.ast.cam.ac.uk/alerts>

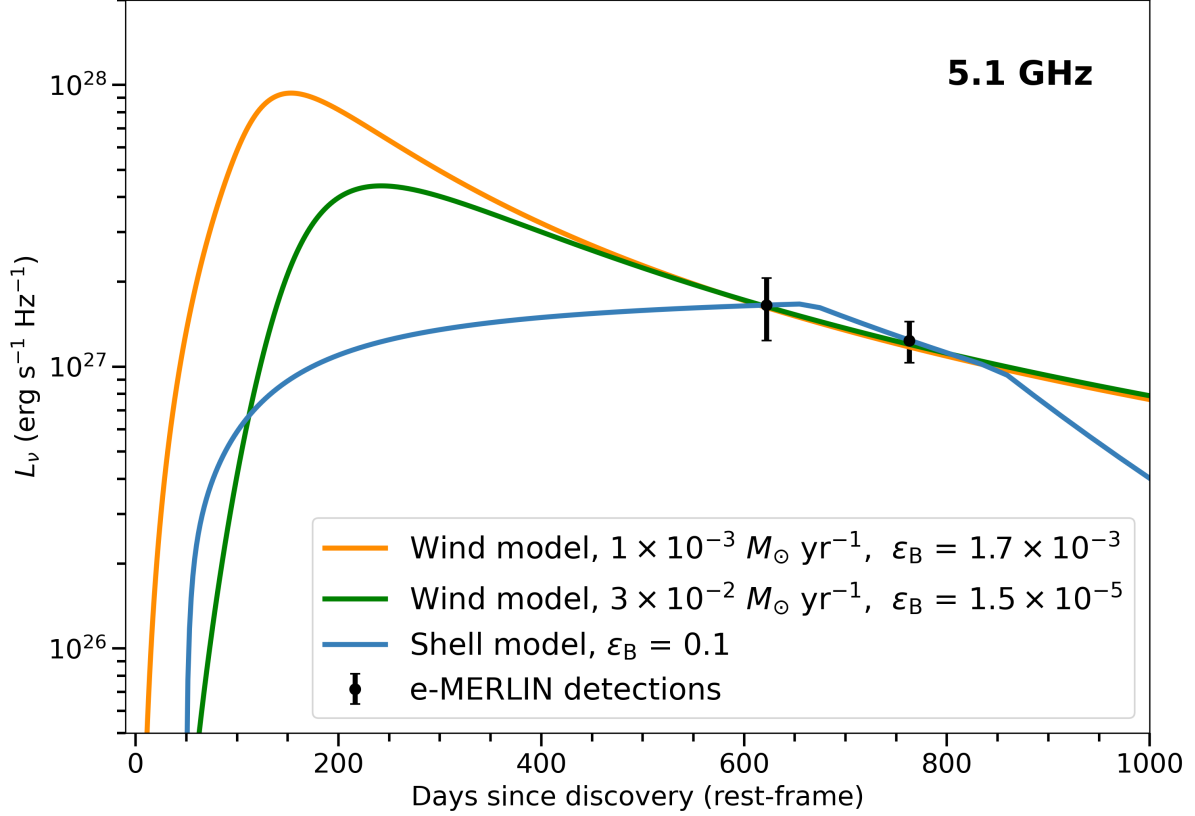


**Fig. 2. The radio detections of SN 2020eyj at 5.1 GHz can be reconciled with CSM interaction.** For the wind model, where the CSM follows a density profile of  $\rho \propto r^{-2}$  (Moriya et al. (2019)), we assume a pre-SN wind velocity of  $1000 \text{ km s}^{-1}$  and adopt a mass-transfer rate as inferred from fitting the bolometric light curve of SN 2020eyj. Depending on the level of line of sight extinction affecting the bolometric light curve, the wind model fits the observations well for the microphysics parameter  $\epsilon_B = 1.7 \times 10^{-3}$  ( $1.5 \times 10^{-5}$ ), and a CSM mass of  $M_{\text{CSM}} = 0.3 M_{\odot}$  ( $1 M_{\odot}$ ) within  $10^{17} \text{ cm}$  when  $E(B-V) = 0 \text{ mag}$  ( $0.5 \text{ mag}$ ). For the shell model (Harris et al., 2016, 2021), where the CSM is concentrated in a constant density CSM shell, we assume  $\epsilon_B = 0.1$ , and obtain a best estimate for the CSM mass of  $M_{\text{CSM}} = 0.36 M_{\odot}$  and a CSM interaction end time of  $t_{\text{end}} = 665 \text{ days}$  (a width of  $8.6 \times 10^{16} \text{ cm}$ ). In both the wind and shell model fits,  $\epsilon_e = 0.1$  is assumed. From Kool et al. (2023)

the *Gaia* position, we interpret the compact radio source as the likely radio counterpart of SN 2020eyj.

### 3. Radio light curve modeling

We explored two fundamental configurations to model the synchrotron emission generated by the shock interaction between the ejecta and circumstellar medium (CSM): a constant density shell and a wind-like density profile characterized by  $\rho \propto r^{-2}$  (Fig. 2). These configurations represent distinct physical scenarios: the constant density shell could arise from discrete mass ejection events such as novae, while the wind-like CSM profile would be characteristic of an optically thick wind regime. In the latter case, the mass-transfer rate from the donor star to the white dwarf (WD) exceeds the maximum accretion rate at which Herich material can be efficiently burned on the WD surface (Nomoto, 1982; Hachisu et al., 1999; Moriya et al., 2019).

For the shell configuration, our analysis indicates that the observed radio emission is optimally reproduced with

a CSM mass of  $M_{\text{CSM}} = 0.36 M_{\odot}$ . This model predicts a steep decline in the radio light curve beginning around 900 days. In contrast, the wind model, assuming a pre-SN wind velocity of  $1000 \text{ km s}^{-1}$ , successfully reproduces both the bolometric light curve tail (Kool et al., 2023) and radio detections with the following parameters: a mass-transfer rate of  $10^{-3} - 10^{-2} M_{\odot} \text{ yr}^{-1}$ , microphysics parameter  $\epsilon_B$  ranging from  $10^{-5}$  to  $10^{-3}$ , and a CSM mass between  $0.3$  and  $1.0 M_{\odot}$  within a radius of  $10^{17} \text{ cm}$ . The precise CSM mass estimate depends on the line-of-sight extinction affecting the tail phase of SN 2020eyj.

The shell and wind models exhibit distinct evolutionary behaviors in their radio light curves (Fig. 2), particularly during early phases where the wind model predicts a significantly earlier peak compared to the shell model. While no radio observations were available during these early epochs, extended multi-frequency radio monitoring beyond 1000 days will be crucial for discriminating between these scenarios. Such observations would reveal either the sharp decline characteristic of the shell model

or the more gradual fade expected from a wind-like CSM profile.

#### 4. Conclusions

Our observations of SN 2020eyj offer evidence for the He star + WD formation channel (Kool et al., 2023), and makes this the first SN Ia in which CSM interaction is confirmed through the detection of a radio counterpart. It is unclear how representative SN 2020eyj is, as monitoring usually stops after a seemingly normal SN Ia has been classified. The unusual properties of SN 2020eyj were only noted by virtue of its relatively near distance, which allowed for the detection of the unusual light curve tail, and the efforts of ZTF to classify every transient brighter than 19th magnitude. This first radio detection opens the possibility to use radio campaigns to reveal the structure of the CSM around other SN Ia, and sets a time scale in which radio searches can be fruitful. Targeted observations on known and future SN Ia may show radio observations as a robust tool to unveil the nature of the progenitor of this type of SN Ia. This will be specially relevant in the context of large radio surveys like VLASS, LoTSS and eventually the SKA. High-angular resolution, including VLBI, will play a critical role to facilitate cross-identification of radio counterparts of known SN Ia, in particular when diffuse contamination from the host galaxy is significant.

*Acknowledgements.* J.M. and M.A.P.-T. acknowledge financial support from the Severo Ochoa grant CEX2021-001131-S and from the National grant PID2023-147883NB-C21, funded by MCIU/AEI/ 10.13039/501100011033. We acknowledge the Spanish Prototype of an SRC (SPSRC) service and support funded by the Ministerio de Ciencia, Innovación y Universidades (MICIU), by the Junta de Andalucía, by the European Regional Development Funds (ERDF) and by the European Union NextGenerationEU/PRTR. The SPSRC acknowledges financial support from the Agencia Estatal de Investigación (AEI) through the "Center of Excellence Severo Ochoa" award to the Instituto de Astrofísica de Andalucía (IAA-CSIC) (SEV-2017-0709) and from the grant CEX2021-001131-S funded by MICIU/AEI/ 10.13039/501100011033. e-MERLIN is a National Facility operated by the University of Manchester at Jodrell Bank Observatory on behalf of STFC. The National Radio Astronomy Observatory is a facility of the National Science Foundation operated under cooperative agreement by Associated Universities, Inc.

#### References

- Dilday, B., Howell, D. A., Cenko, S. B., et al. 2012, *Science*, 337, 942
- Hachisu, I., Kato, M., Nomoto, K., et al. 1999, *ApJ*, 519, 314
- Harris, C. E., Chomiuk, L., & Nugent, P. E. 2021, *ApJ*, 912, 23
- Harris, C. E., Nugent, P. E., & Kasen, D. N. 2016, *ApJ*, 823, 100
- Kool, E. C., Johansson, J., Sollerman, J., et al. 2023, *Nature*, 617, 477

- Lundqvist, P., Kundu, E., Pérez-Torres, M. A., et al. 2020, *ApJ*, 890, 159
- Moldón, J. 2021, *Astrophysics Source Code Library*. ascl:2109.006
- Moriya, T. J., Liu, D., Wang, B., et al. 2019, *MNRAS*, 488, 3949
- Nomoto, K. 1982, *ApJ*, 253, 798
- Offringa, A. R., McKinley, B., Hurley-Walker, N., et al. 2014, *MNRAS*, 444, 606
- Pérez-Torres, M. A., Lundqvist, P., Beswick, R. J., et al. 2014, *ApJ*, 792, 38
- Wang, B., Chen, X., Meng, X., et al. 2009, *ApJ*, 701, 1540